

Received:  
9 November 2018  
Revised:  
26 February 2019  
Accepted:  
8 March 2019

Cite as: Omar Dagdag,  
Ahmed El Harfi,  
Mustapha El Gouri, Zaki Safi,  
Ramzi T. T. Jalgham,  
Nuha Wazzan,  
Chandrabhan Verma,  
E. E. Ebeno,  
U. Pramod Kumar.  
Anticorrosive properties of  
Hexa (3-methoxy propan-1,2-  
diol) cyclotri-phosphazene  
compound for carbon steel in  
3% NaCl medium: gravimetric,  
electrochemical, DFT and  
Monte Carlo simulation studies.  
*Heliyon* 5 (2019) e01340.  
doi: 10.1016/j.heliyon.2019.  
e01340



# Anticorrosive properties of Hexa (3-methoxy propan-1,2-diol) cyclotri-phosphazene compound for carbon steel in 3% NaCl medium: gravimetric, electrochemical, DFT and Monte Carlo simulation studies

Omar Dagdag <sup>a,\*</sup>, Ahmed El Harfi <sup>a</sup>, Mustapha El Gouri <sup>b</sup>, Zaki Safi <sup>c,\*\*</sup>,  
Ramzi T. T. Jalgham <sup>d</sup>, Nuha Wazzan <sup>e</sup>, Chandrabhan Verma <sup>f,g</sup>, E. E. Ebeno <sup>f,g</sup>,  
U. Pramod Kumar <sup>h</sup>

<sup>a</sup> Laboratory of Agroresources, Polymers and Process Engineering, Department of Chemistry, Faculty of Science, Ibn Tofail University, BP 133, 14000 Kenitra, Morocco

<sup>b</sup> Laboratory of Process, Renewable Energy and Environment, Department of Process Engineering, Height School of Technology, Sidi Mohammed Ben Abdallah University, P.O. Box 2427, 30000, Fez, Morocco

<sup>c</sup> Al Azhar University-Gaza, Chemistry Department, Faculty of Science, P.O Box 1277, Gaza, Palestine

<sup>d</sup> Department of Oil and Gas, Faculty of Engineering, Bani Walid University, Bani Walid, Libya

<sup>e</sup> King Abdulaziz University, Chemistry Department, Faculty of Science, P.O Box 42805, Jeddah, 21589, Saudi Arabia

<sup>f</sup> Material Science Innovation & Modelling (MaSIM) Research Focus Area, Faculty of Natural and Agricultural Sciences, North-West University, Private Bag X2046, Mmabatho, 2735, South Africa

<sup>g</sup> Department of Chemistry, Faculty of Natural and Agricultural Sciences, School of Chemical and Physical Sciences, North-West University, Private Bag X2046, Mmabatho 2735, South Africa

<sup>h</sup> Department of Chemistry SRM Research Institute, SRM Institute of Science and Technology, Kattankulathur, Chennai, 603203, India

\* Corresponding author.

\*\* Corresponding author.

E-mail addresses: [omar.dagdag@uit.ac.ma](mailto:omar.dagdag@uit.ac.ma) (O. Dagdag), [z.safi@alazhar.edu.ps](mailto:z.safi@alazhar.edu.ps) (Z. Safi).

## Abstract

The corrosion inhibition performance of Hexa (3-methoxy propan-1,2 diol) cyclotriphosphazene (HMC) on carbon steel in 3% NaCl solution was investigated by weight loss (WL), potentiodynamic polarization (PDP), electrochemical impedance spectroscopy (EIS) measurements, Density functional theory (DFT) and Monte Carlo (MC) simulation. The corrosion inhibition efficiency at optimum concentration ( $10^{-3}$ M) is 99% of HMC at 298 K. The corrosion inhibition efficiency at  $10^{-3}$  M decreases with increase in temperature. The adsorption of HMC on the surface of carbon steel obeyed Langmuir isotherm. Potentiodynamic polarization study confirmed that inhibitor anodic-type. DFT and Monte Carlo (MC) simulations based computational approaches were undertaken to support the experimental findings. DFT studies revealed that HMC interact with metallic surface through donor-acceptor interactions in which the anionic parts act as electron donor (HOMO) and cationic parts behaved as electron acceptor (LUMO). The MC simulations study showed that studied HMC adsorb spontaneously on Fe (110) surface.

Keywords: Materials chemistry, Theoretical chemistry, Inorganic chemistry

## 1. Introduction

Steel alloys are widely utilized in many applications including petroleum industries, especially carbon steel are prone to corrosion when they come into contact with corrosive materials, especially in an environment containing  $\text{Cl}^-$  ions. Presence of  $\text{Cl}^-$  ion on the metallic surface initiates the formation of metal oxides; thereby adversely affect the physiochemical properties of the metals. The use of corrosion inhibitors, mainly heterocyclic compounds have been reported to be one of the most effective methods for against corrosion because they can easily adsorb on metallic surface via their molecular structures P, O, S, N,  $\pi$ -electrons and aromatic rings [1, 2, 3, 4, 5]. Many of these heterocyclic compounds are obtained efficiently using easy-access synthesis pathways and are usually used at lower concentrations during the corrosion inhibition process [6, 7, 8]. Among this group of heterocyclic compounds, we find Hexachlorocyclotriphosphazene. Hexachlorocyclotriphosphazene are an important group containing the formula  $(\text{NPCl}_2)_3$ . The molecule has a cyclic backbone consisting of alternating P and N atoms. They have active phosphorus-halogen bonds that can be replaced with nucleophiles, leading to the formation of different types of product [9, 10, 11]. Cyclotriphosphazene is well established nitrogen rich ring containing molecule with three additional nitrogen atoms those can easily protonate and enhance the solubility of polar solvents. Recently, derivatization of cyclotriphosphazene gained the significant advanced for variety of purposes including corrosion inhibition. Cyclotriphosphazene have been investigated as effective corrosion

inhibitors for metals and alloys in aggressive solutions owing to their high protection ability which is in turn attributed to the adsorption of these compounds by their non-bonding electrons of nitrogen atoms and  $\pi$ -electrons of three double (-P=N-) bonds. In this study demonstrated the effect of cyclotriphosphazene derivative designated as Hexa (3-methoxy propan-1,2-diol) cyclotriphosphazene (HMC) having either six identical oxygen containing 3-methoxy propan-1,2 diols. Last decade has witnessed a dramatic increase of using Density Functional Theory methods (DFT) to magnificently define the chemical reactivity of inhibitors and their adsorption competence on metal surface [12, 13, 14, 15, 16, 17, 18]. Such computations have been widely used to analyze the molecular electronic structures of adsorption-type inhibitors using a number of quantum chemical descriptors which gives important insights on corrosion inhibition mechanisms. Coupled with the fact that metal inhibitor interactions can be best describe with the aid of the Hard and Soft Acid and Bases (HSAB) principle [19], where organic inhibitors can be regarded as Lewis bases that offer unshared non-bonding and  $\pi$ -electrons to the empty d-orbitals of the iron atoms that acted as electron acceptor (Lewis acid). Therefore, inhibition behavior of the organic inhibitors including HMC is largely influenced by the electronic properties of the inhibitor molecules. Monte Carlo (MC) simulation has been another effective tool to study the interaction of inhibitors with the metal surface or similar problems.

In view of this, present investigation deals with the implementation of one cyclotriphosphazene derivatives synthesized by condensation of Hexachlorocyclotriphosphazene and 2,3-epoxy-1-propanol and demonstrated as corrosion inhibitor for marine-environment (3% NaCl) corrosion of carbon steel. Several commonly employed methods such as chemical (weight loss), electrochemical impedance spectroscopy (EIS), and potentiodynamic polarization (PDP) have been undertaken to study the inhibition ability of the Hexa (3-methoxy propan-1,2-diol) cyclotriphosphazene (HMC). The adsorption and inhibition behavior of HMC were supported by density functional theory (DFT) based quantum chemical calculations method. A significant correlation among the parameters of experimental and theoretical methods has been achieved in present study. The most stable configuration and adsorption energies for the interaction of the inhibitor with Fe (110) surface were studied by Monte Carlo simulation.

## 2. Experimental

### 2.1. Materials

Carbon steel specimens were used as working (test) material. The corrosive medium of 3% NaCl concentration was manufactured by dilution with distilled water. The inhibition effect of HMC was tested at four different concentrations denoted by,  $10^{-3}$ ,  $10^{-4}$ ,  $10^{-5}$  and  $10^{-6}$  M. The inhibitor, HMC was synthesized according a reported procedure [6]. In brief, a mixture of an (2,3-epoxy-1-propanol) (2) compound

(2g) and toluene (14.25mL) containing 2.22 g of triethyl amine at room temperature. The mixture was cooled (ice-water). After was added 1.5 g of hexachloro cyclotriphosphazene (1) and toluene (7.5 mL) in two-necked round bottom flask, fitted with a condenser and a magnet stir bar was added drop wise for 3 h. After the addition was completed, the stirring was continued again for another 45 h at room temperature. The residual solvent was removed using a rotary evaporator in order to obtain the desired brown viscous solution of resin (3). After we take 5 g of product obtained epoxy resin (ER) (3) and added 10 mL of basic solution containing 2.1 g of NaOH. The mixture was neutralized, filtered and dried by  $\text{Na}_2\text{SO}_4$  and to remove water.

Schematic diagram for the preparation of the HMC is shown in Fig. 1.

The structure of the produced was verified by  $^1\text{H}$  NMR and FT-IR spectroscopic characterization techniques. HMC: brown solid product, very soluble in water, yield 95%;  $^1\text{H-NMR}$  ( $\text{CDCl}_3$ , 300 MHz):  $\delta$  ppm = 2.7 (dd, 2H, -O-CH<sub>2</sub>), 3.38 (m, 1H, CH), 4 (dd, 2H, CH<sub>2</sub>).  $^{31}\text{P-NMR}$ :  $\delta$  ppm = 9.32 (s). FTIR ( $\text{cm}^{-1}$ ): 1266 and 1200 (P=N stretching), 1013 (P-O-C), 2927, 2965 (asymmetric and symmetric  $\gamma$  of C-H units), 2800, 3600 (-OH).

## 2.2. Methods

### 2.2.1. Weight loss measurements

The weight loss analysis was carried out using the carbon steel of previously reported composition and procedure as described in our earlier studies [20, 21]. The gravimetric parameters were derived using following equations [22]:

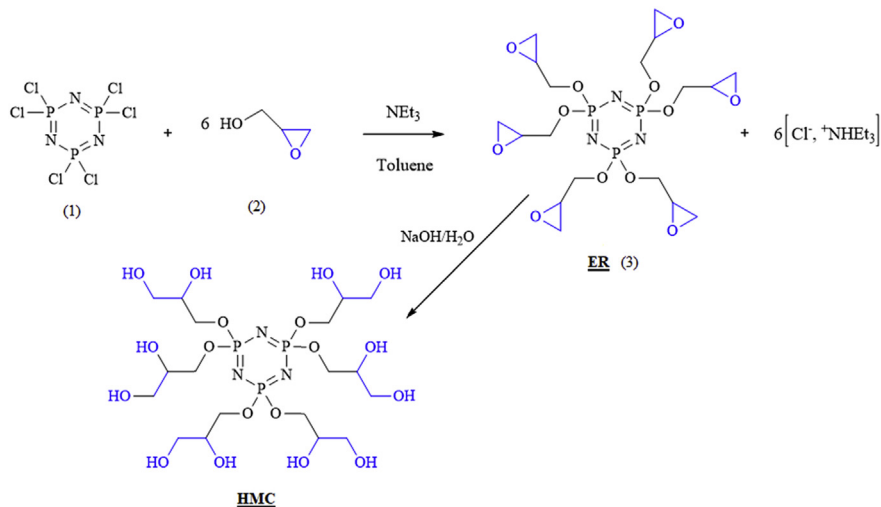


**Fig. 1.** A representative scheme showing the total synthesis of Hexa (3-methoxy propan-1,2-diol) cyclotriphosphazene (HMC).

$$W_{\text{corr}} = \frac{W_0 - W_i}{St} \quad (1)$$

$$\theta = \frac{W_0 - W_i}{W_0} \quad (2)$$

$$\eta_{\text{WL}} = \frac{W_0 - W_i}{W_0} \times 100 \quad (3)$$

where  $W_0$  and  $W_i$  represent the weight loss values without and with HMC, respectively,  $t(h)$  is the immersion time and  $S$  is the total surface area of the metal sample.

### 2.2.2. Electrochemical measurements

Instruments and experimental procedures were similar as described in our previous reported literatures [23, 24, 25].

From EIS and polarization techniques, inhibition effect of HMC was evaluated using Eqs. (4) and (5).

The inhibition efficiency  $\eta_{\text{EIS}}\%$  is calculated from resistance polarization  $R_p$  of HMC given by Eq. (5):

$$\eta_{\text{EIS}}(\%) = \frac{R_p - R_p^0}{R_p} \times 100 \quad (4)$$

$$\eta_{\text{PDP}}\% = \left(1 - \frac{i_{\text{corr}}}{i_{\text{corr}}^0}\right) \times 100 \quad (5)$$

where,  $R_p^0$  and  $R_p$  represent the resistance polarization values without and with HMC, respectively. Whereas,  $i_{\text{corr}}^0$  and  $i_{\text{corr}}$  represent the corrosion current density values without and with the inhibitor respectively.

### 2.2.3. Computational details

DFT on the HMC in its neutral as well as solvated phase was carried out using Gaussian 09 similar to our previously reported procedures [26, 27, 28, 29, 30, 31, 32, 33].

Several DFT parameters were computed using following relationships [34, 35, 36, 37, 38, 39, 40, 41, 42, 43, 44, 45, 46, 47, 48]: As per the theorem of Koopman, the values of frontier molecular orbitals can be correlated with ionization potential (I) as well as electron affinity (A) as per the Eqs. (6) and (7). The energies the energies are highest occupied molecular orbital ( $E_{\text{HOMO}}$ ) and lowest unoccupied molecular orbital ( $E_{\text{LUMO}}$ ) and energy gap ( $\Delta E = E_{\text{LUMO}} - E_{\text{HOMO}}$ ) have been calculated. Employing the magnitude of A and I, several other DFT indices like electronegativity ( $\chi$ ), global harness ( $\eta$ ) and softness ( $\sigma$ ) were computed for the forms of

HMC as per the Eqs. (8)–(10). It is well documented that metal inhibitor bindings involve donor-acceptor phenomenon. The fraction of electron transfer ( $\Delta N$ ) by HMC molecules was computed as per the Eq. (11). Which is the initial molecule-metal interaction energy ( $\Delta\psi$ ) and the inhibitor molecule and the metal surface as per the Eqs. (12) and (13).

$$I = -E_{\text{HOMO}}; \quad (6)$$

$$A = -E_{\text{LUMO}}; \quad (7)$$

$$\chi = \frac{I + A}{2}; \quad (8)$$

$$\eta = \frac{I - A}{2} \quad (9)$$

$$\sigma = \frac{1}{\eta} \quad (10)$$

$$\Delta N = \frac{\varphi_{Fe} - \chi_{inh}}{2(\eta_{Fe} + \eta_{inh})} \quad (11)$$

$$\Delta\psi = \frac{(\chi_{Fe} - \chi_{inh})^2}{2(\eta_{Fe} + \eta_{inh})} \quad (12)$$

$$\Delta E_{\text{back-donation}} = -\frac{\eta}{4} \quad (13)$$

Where, where  $\phi$  corresponds to the work function, which is used as the appropriate measure of electronegativity of iron, and  $\eta_{Fe} = 0$ . The theoretical value of  $\phi$  is 4.82 eV for Fe (110) plan which is reported to have the higher stabilization energy. Eq. 13 implies that when  $\eta > 0$  or  $\Delta E_{\text{b-d}} < 0$ , back-donation from the molecule to metal is energetically favored.

It is very necessary to identify the reactive centres present within the inhibitor molecules. The Fukui Indices (FIs) analyses help to determine and recognize the sites of the molecule which are responsible for nucleophilic or electrophilic reactions. The presence of the nucleophilic or electrophilic center facilitates the interaction of the inhibitor molecules with the surface atoms of the metal.

Fukui functions for nucleophilic and electrophilic attacks are obtained from finite difference approximations as the follows:

$$f_k^+(r) = \rho_k(N+1) - \rho_k(N) \quad \text{For nucleophilic attack} \quad (14)$$

$$f_k^-(r) = \rho_k(N) - \rho_k(N-1) \quad \text{For electrophilic attack} \quad (15)$$

$\rho_k(N), \rho_k(N-1)$  and  $\rho_k(N+1)$  are the gross electronic populations of the site  $k$  in neutral, cation and anion, respectively.

Monte Carlo simulations help us to find the most stable adsorption sites on metal and metal oxide surfaces through finding the low energy adsorption sites on both periodic and non-periodic substrates or to investigate the preferential adsorption of mixtures of adsorbate components. In order to investigate the most suitable adsorption modes for the neutral inhibitor, the HMC molecule and  $\text{Fe}_2\text{O}_3$  surface were prepared. In this study, the HMC molecule was drawn and the hydrogens were adjusted, then the molecules were cleaned using sketch tools available in the Materials Visualizer. The sketched and fully optimized geometry structure of HMC is shown in Fig. 8. The molecule that are shown in Fig. 8 were optimized (i.e., energy minimizing) in the Monte Carlo simulations using the forcite module and the Condensed- Phase Optimized Molecular Potentials for Atomistic Simulation Studies (COMPASS) force field. For cite is an advanced classical mechanics tool that allows energy calculations and geometry optimizations. COMPASS force field which used to optimize the structures the HMC of all components of the system of interest ( $\text{Fe}^+$  inhibitor) and represents a technology break-through in force field method. COMPASS is the first ab initio force field that enables accurate and simultaneous prediction of chemical properties (structural, conformational, vibrational, etc.) and condensed-phase properties (equation of state, cohesive energies, etc.) for a broad range of chemical systems. It is also the first high quality force field to consolidate parameters of organic and inorganic materials. Materials Studio provides the unit cell structures of metal oxides with the associated experimental lattice parameters. Metal oxide surfaces were prepared by employing the desired cleavage planes  $h\bar{k}\ell$  (110). Using the surface builder module of Materials Studio. The Metal oxide surface must be large enough to accommodate the inhibitor molecules; therefore, the constructed surface was enlarged by periodic replication to triple  $U \times V$  ( $3 \times 3$ ) in order to expose a more realistic surface area for docking the inhibitor molecules. The surface with parameters of 45.7 and 27.9 Å was produced. It is important that the size of the vacuum is great enough such that the non-bonded calculation for the adsorbate does not interact with the periodic image of the bottom layer of atoms in the surface; thus, a vacuum slab with thickness 31.7 Å was built using Crystal Builder. A low-energy adsorption site is identified by carrying out a Monte Carlo search. This process is repeated to identify further local energy minima. During the course of the simulation, adsorbate molecule are randomly rotated and translated around the substrate. The configuration that results from one of these steps is accepted or rejected according to the selection rules of the Metropolis Monte Carlo method. The Monte Carlo (MC) simulation was performed using Materials Studio 5.5 program [49, 50, 51, 52, 53].

### 3. Results and discussion

#### 3.1. Weight loss measurements (WL)

The WL parameters derived for steel corrosion after 24 h immersion time in 3 % NaCl solution is listed in [Table 1](#). Visualization of the results showed that inhibition performance of HMC is concentration dependent it increases on increasing the concentration of HMC and maximum efficiency was observed at  $10^{-3}$  M. The increase in the inhibition effectiveness of HMC with their concentration is might be attributed to the increase in surface coverage values at higher concentrations.

The process of corrosion inhibition was highly influenced by the temperature. For the purpose of further understanding the effect of temperatures, the corrosion inhibition ability of HMC in 3% NaCl solution was studied at various temperatures in the rang 298–328 K for 24 h of immersion. The evolution of  $W_{corr}$  and  $\eta_{WL}$  with various temperature for carbon steel in 3% NaCl solution in the without and with addition  $10^{-3}$  M of HMC is given in [Table 2](#).

The results indicate that the values of  $\eta_{WL}$  obtained from the weight loss for carbon steel corrosion in 3% NaCl solution in the without and with addition  $10^{-3}$  M of HMC at different temperatures decreased with increasing temperature. The maximum value of  $\eta_{WL}\%$  obtained for  $10^{-3}$  M of HMC is 96 % at 298 K. This behavior indicates desorption of inhibitor molecule.

#### 3.2. Potentiodynamic polarization measurements (PDP)

The PDP curves for carbon steel in 3 % NaCl are shown in [Fig. 2](#). Parameters are presented in [Table 3](#). Carbon steel readily undergoes anodic metallic dissolution and cathodic hydrogen evolution reactions using following schemes.

Anodic dissolution reactions [\[54\]](#):

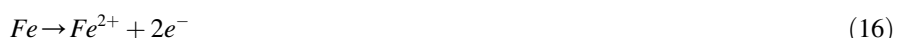


**Table 1.**  $W_{corr}$  and  $\eta_{WL}$  obtained from weight loss measurements for carbon steel in 3% NaCl with and without various concentration of HMC at 298 K for 24 h.

Inh	C (M)	$W_{corr}$ (mg/cm <sup>2</sup> h <sup>1</sup> )	$\eta_{WL}(%)$
Blank	—	3	—
HMC	$10^{-6}$	0.23	92
	$10^{-5}$	0.22	93
	$10^{-4}$	0.17	94
	$10^{-3}$	0.12	96

**Table 2.** Effect of temperature on the corrosion rate ( $W_{corr}$ ) and corrosion current densities ( $i_{corr}$ ) for carbon steel in 3% NaCl solution in the absence and addition  $10^{-3}$  M of HMC.

T (K)	$W_{corr}$ (mg/cm <sup>2</sup> h <sup>1</sup> )		$i_{corr}$ μA/Cm <sup>2</sup>		$\eta_{WL}$ (%)	$\eta_{PDP}$ (%)
	Blank	$10^{-3}$ M of HMC	Blank	$10^{-3}$ M of HMC	—	—
298	3	0.12	280	3	96	99
308	5.51	0.41	345	23.4	92	93
318	8.89	1.31	556	85.8	85	85
328	11.45	2.05	706	137.5	82	80



Cathodic hydrogen evolution reactions:



However, in its presence HMC forms protective inhibitive barrier which separates metal from the aggressive 3 % NaCl solution and protect from corrosion.

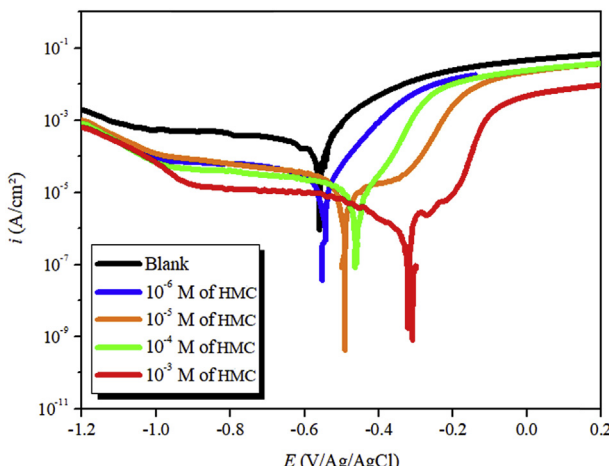


**Fig. 2.** PDP curves for carbon steel corrosion in 3% NaCl solution containing different concentrations of HMC.

**Table 3.** PDP parameters for carbon steel corrosion in 3% NaCl solution with and without addition of different concentrations of HMC.

Inh	C (M)	$E_{corr}$ (mV/Ag/AgCl)	$i_{corr}$ ( $\mu A/cm^2$ )	$\beta_a$ ( $V^{-1}$ )	$-\beta_c$ ( $V^{-1}$ )	$\eta_{PDP}\%$
Blank	—	−559	280	0.12	0.12	—
	$10^{-6}$	−552	40	0.26	0.19	85
HMC	$10^{-5}$	−498	27	0.22	0.18	90
	$10^{-4}$	−463	14	0.29	0.16	94
	$10^{-3}$	−320	3	0.26	0.03	99

From the results obtained, the consequences is was perceived that  $i_{corr}$  on the two cathodic and anodic polarization branches decrease in the presence of the HMC. Correspondingly, the inhibition efficacy increases by increasing the concentration of the HMC. The maximum efficiency of 99 % was obtained at  $10^{-3}$  M. Furthermore, as shown in Fig. 2 and Table 3, with the addition of HMC molecules shifts corrosion potential is shifted to more anodic potential and also shows a significant change the anodic polarization branches. Anodic dominance of the HMC can be easily observed from the results presented in the table [55]. These results suggest that HMC molecules reduces the anodic metallic dissolution and retards the reduction of oxygen.

The influence of temperature on the various corrosion parameters  $i_{corr}$  and  $\eta_{PDP}\%$  obtained from the PDP of carbon steel was studied in 3% NaCl solution in the temperature rang (298–328 K)without and with addition  $10^{-3}$  M of HMC. Results are listed in Table 2.

From the results of Table 2 shown that, as the temperature increased in in 3% NaCl solution in the without and with addition  $10^{-3}$  M of HMC, the values of  $i_{corr}$  increase and  $\eta_{PDP}\%$  decrease. This result can be explaining by desorption of HMC molecules from carbon steel surface.

### 3.3. Electrochemical impedance spectroscopy measurements

Nyquist plots for the carbon steel electrode in 3% NaCl solution and containing various concentrations of HMC after 30 min of immersion time are presented in Fig. 3.

It can be seen that in the absence of inhibitor, Nyquist plot contain only one semi-circle. This indicates that corrosion on the carbon steel surface is mainly controlled by the charge transfer process [56, 57]. In Nyquist plot, difference in the lower frequency and higher frequency in the real axis is generally considered as charge transfer resistance ( $R_{ct}$ ). The charge transfer resistance must be consistent with the resistance between metal and Outer Helmholtz Plane (OHP). Thus, the resistance

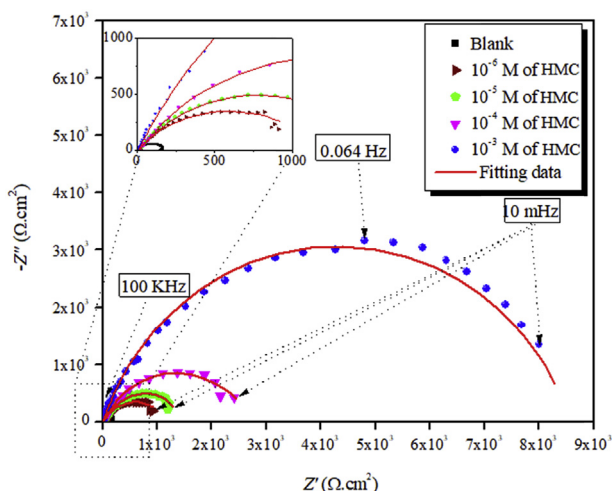


**Fig. 3.** Nyquist diagrams for carbon steel in 3% NaCl solution containing different concentrations of HMC.

coming from the metal/solution interface in absence of the inhibitor is mainly due to the charge transfer resistance ( $R_{ct}$ ), diffuse layer resistance ( $R_d$ ) and accumulation resistance ( $R_a$ ). Therefore, along with  $R_{ct}$ ,  $R_d$  and  $R_a$  have to be taken in account. Thus, difference in the lower frequency and higher frequency in the real axis is considered as polarization resistance ( $R_p$ ). It is also seen from the Nyquist plot that the diameter of semi-circle is concomitantly increased in the presence of the inhibitor. This phenomenon suggests the formation of protective layer on the metal surface. Thus, in presence of inhibitor film resistance ( $R_f$ ) have to be considered in the polarization resistance ( $R_p$ ). So, in presence of inhibitor,  $R_p$  is designated as  $\Sigma (R_{ct} + R_d + R_a + R_f)$ . The addition of HMC to the aggressive solution leads to a change of the impedance diagrams in both shape and size, which a depressed semi-circle at the high frequency part of the spectrum was observed and a second time constant appeared at low frequency region. The first capacitive loop appearing at high frequency region was attributed to the charge transfer resistance and the diffuse layer resistance, the second one at low frequencies related to the adsorption of inhibitor molecules on the metal surface and all other accumulated kinds at the metal/solution interface (inhibitor molecules, corrosion products, etc.). As seen from Fig. 3, the  $R_p$  values increased with the HMC concentration, which can be attributed to the formation of a protective over layer at the metal surface, which becomes a barrier for the mass and the charge transfers. The double layer can be represented by the electrical equivalent circuit diagrams to the model metal/solution interface. The corresponding electrical equivalent circuit model for the carbon steel in uninhibited solution is given in Fig. 4c with a schematic representation of the potential distributions on the metal/solution interface (Fig. 4a) and the resistances related to the double layer (Fig. 4b). According to Fig. 4, the  $R_p$  includes the  $R_{ct}$ , the  $R_d$  and all the other accumulated kinds of ions, corrosion products, etc. at metal/solution interface.

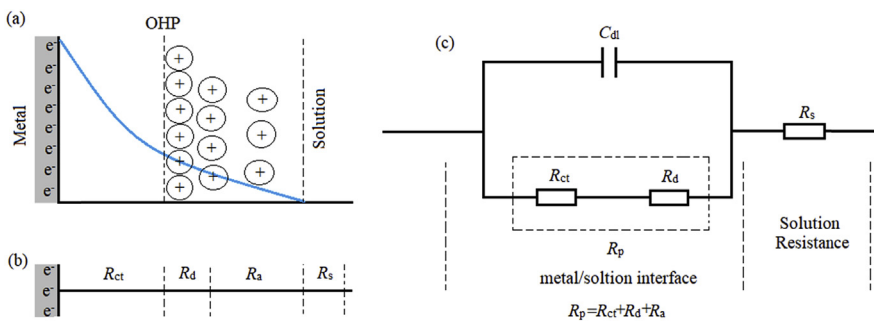


**Fig. 4.** The potential distributions on the metal/solution interface (a), the resistances related double layer (b), and proposed electrical equivalent circuit diagram for blank solution (c).

The  $R_{ct}$  must be corresponded to the resistance between the metal and OHP (outer Helmholtz plane). All the other resistances must be considered as the simple resistance on the current crossing away. In the case of the inhibited solutions, related electrical equivalent circuit model is given in Fig. 5b with a schematic representation of metal/solution interface (Fig. 5a) [58, 59, 60].

The obtained Nyquist plots have been fitted using these equivalents circuits where the constant phase element and the polarization resistance are in parallel combination and these two are connected in series with the electrolyte resistance ( $R_s$ ). The constant phase element is defined by the following Eq. (23) [59]:

$$Z_{CPE} = \frac{1}{Q(i\omega)^n} \quad (23)$$

Where,  $Q$  is the proportionality coefficient,  $\omega$  represents angular frequency,  $i$  is the imaginary unit and  $n$  is a measure of surface irregularity. For whole number of  $n = 1, 0, -1$ , CPE represent a capacitance ( $C$ ), resistance ( $R$ ) and inductance, respectively.

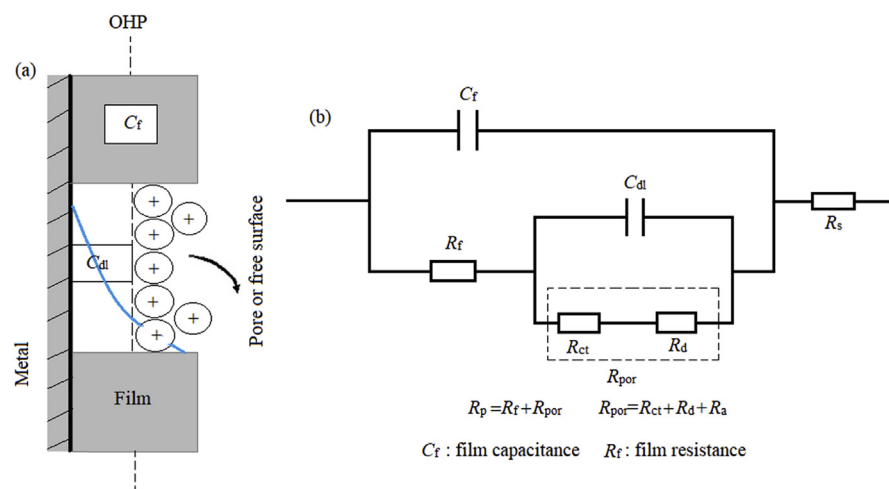


**Fig. 5.** Schematic representation of metal/inhibitor/solution interface (a) and proposed equivalent electrical circuit diagram for EIS results of the carbon steel in inhibited solutions (b).

A direct correlation between the polarization resistance and double layer capacitance ( $C_{dl}$ ) at the metal/solution interface is obtained by the following Eq. (24):

$$C_{dl} = \left( \frac{Q}{R_p^{n-1}} \right)^{1/n} \quad (24)$$

The electrochemical parameters values are listed in Table 4. Results depicted in Table 4 shows that  $R_p$  value increases with increasing the concentration of HMC. It may suggest that a protective layer has been formed on the electrode surface. This layer creates a barrier for charge and mass transfer at the metal-solution interface [59]. It is also observed that with increasing inhibitor concentration the  $C_{dl}$  values are decreased, which can be described by an increase in the thickness of electric double layer or by the decrease of local dielectric constant [59].

### 3.4. Adsorption studies

The adsorption isotherm is frequently utilized to inspect the adsorption mechanism between the inhibitors and metal atoms at the metal surface. The most utilized adsorption isotherm is Langmuir [61]. The Langmuir adsorption isotherm is shown in Eq. (25).

$$\frac{C_{inh}}{\theta} = \frac{1}{K_{ads}} + C_{inh} \quad (25)$$

where  $\theta$  is the surface coverage degree and  $K_{ads}$  is the adsorption process.

Langmuir isotherm and the experimental data have a good linear relationship for the adsorption behavior of the investigated HMC, representing that adsorption of HMC on metallic surface comply with Langmuir adsorption isotherm. The association between  $C_{inh}$  and  $C_{inh}/\theta$  yielded straight lines with intercept of  $K_{ads}$  as shown in Fig. 6. From the  $K_{ads}$  values, the  $\Delta G^\circ_{ads}$  are calculated using Eq. (26) [62]:

**Table 4.** EIS parameters for carbon steel corrosion in 3% NaCl solution with and without addition of different concentrations of HMC.

Inh	$C$ (M)	$R_s$ ( $k\Omega \cdot cm^2$ )	$R_p$ ( $k\Omega \cdot cm^2$ )	$C_{dl}$ ( $\mu F/cm^2$ )	$\eta_{EIS}\%$
Blank	—	10	0.165	—	—
HMC	$10^{-6}$	15	1.0	165	85
	$10^{-5}$	12	1.6	141	90
	$10^{-4}$	12	2.7	68	94
	$10^{-3}$	8	9	52	98

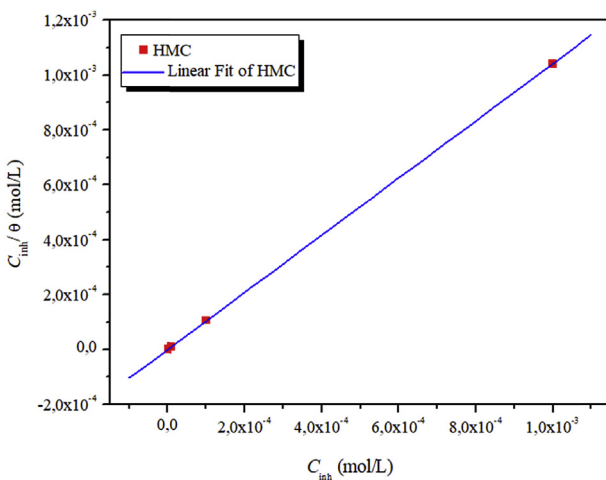


**Fig. 6.** Langmuir adsorption isotherm on weight loss of carbon steel in 3% NaCl solution containing different concentrations of HMC after 24 h at 298 K.

$$K_{ads} = \frac{1}{55.5} \exp\left(\frac{-\Delta G_{ads}^{\circ}}{RT}\right) \quad (26)$$

where  $R$  is the universal gas constant (8.314 J/mol. K), value 55.55 is the water concentration in the solution (mol/L). In general, a high value of  $K_{ads}$  and low value of  $\Delta G_{ads}^{\circ}$  indicating a strong interaction and a strong adsorption on the metal surface [63]. The calculated value of  $K_{ads}$  ( $1.18 \text{ M}^{-1} \times 10^6$ ) and  $\Delta G_{ads}^{\circ}$  ( $-44.57 \text{ kJ mol}^{-1}$ ) indicates that HMC exhibits a strong interactions with carbon steel surface (chemisorption) [64].

### 3.5. Effect of temperature

Generally, increase in the temperature causes significant decrease in the protection ability of the inhibitor molecules. The influence of temperature can be best explained with the aid of Arrhenius Eqs. (27) and (28) [65, 66]:

$$i_{corr} = A \cdot \exp\left(-\frac{E_a}{RT}\right) \quad (27)$$

$$W_{corr} = A \cdot \exp\left(-\frac{E_a}{RT}\right) \quad (28)$$

Arrhenius plots is shown in Fig. 7. Moreover, the Arrhenius equation can be converted Eqs. (29) and (30) (transition state equations) as shown [67, 68]:

$$i_{corr} = \frac{RT}{hN} \exp\left(\frac{\Delta S_a}{R}\right) \exp\left(-\frac{\Delta H_a}{RT}\right) \quad (29)$$

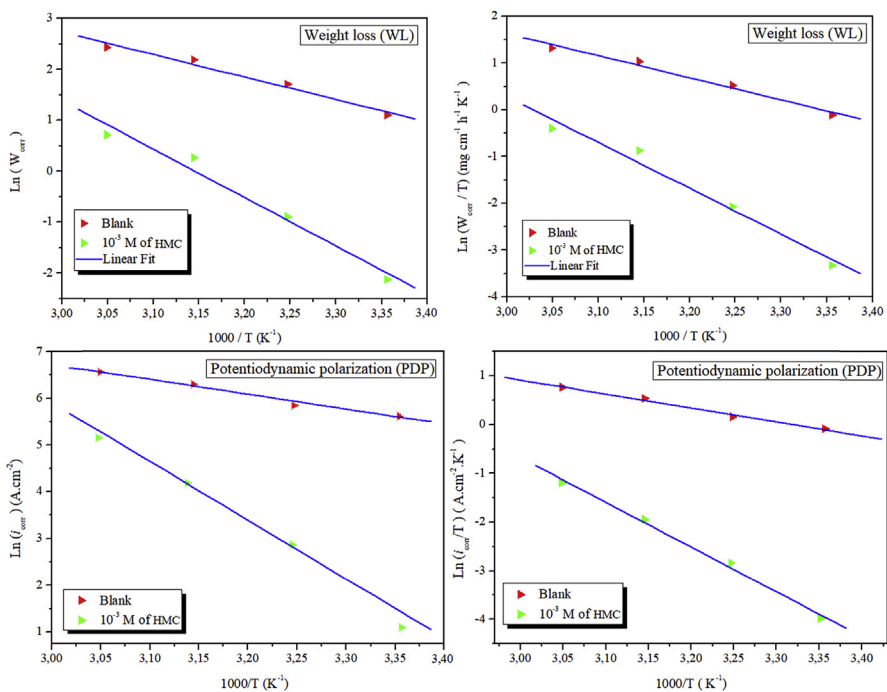


**Fig. 7.** The relationship between  $\ln(W_{\text{corr}})$ ,  $\ln(i_{\text{corr}})$ ,  $\ln(W_{\text{corr}}/T)$  and  $\ln(i_{\text{corr}}/T)$  as a function of  $1/T$  in 3% NaCl solution without and with addition  $10^{-3}$  M of HMC.

$$W_{\text{corr}} = \frac{RT}{hN} \exp\left(\frac{\Delta S_a}{R}\right) \exp\left(-\frac{\Delta H_a}{RT}\right) \quad (30)$$

A is the Arrhenius exponent, T is temperature, N is Avogadro's constant and other symbols have their usual meaning. Several parameters such as  $E_a$ ,  $\Delta H_a$  and  $\Delta S_a$  calculated using Arrhenius and transition state plots (Fig. 7) are presented in Table 5.

The positive value of  $\Delta H_a$  reveals the endothermic nature of metal-inhibitor interactions [69], whereas increased value of  $\Delta S_a$  suggested that replacement of the water molecules from ER that results into the corresponding increase in the disordering (randomness) on the metallic surface.

**Table 5.** Values of  $E_a$ ,  $\Delta H_a$  and  $\Delta S_a$  for carbon steel in 3% NaCl solution without and with addition  $10^{-3}$  M of HMC.

Method	C (M)	$E_a$ (kJ/mol)	$\Delta H_a$ (kJ/mol)	$\Delta S_a$ ( $\text{J} \cdot \text{mol}^{-1} \text{K}^{-1}$ )
WL	Blank	35.82	39.22	-66.06
	$10^{-3}$ M of HMC	78.95	81.52	+49.53
PDP	Blank	26.40	23.82	-118.40
	$10^{-3}$ M of HMC	79.50	76.45	+26.25

### 3.6. Theoretical studies

#### 3.6.1. Quantum chemical calculation

The anticorrosive efficiency of the Hexa (3-methoxy propan-1,2-diol) cyclotriphosphazene (HMC) was investigated by DFT and MC simulations. It is worth mentioning that the corrosion effect of chemical inhibitors is accompanied to its adsorption via electronic interaction with the metal's surface. Recently, quantum chemical calculation has been used to provide the scientists more information about structural properties of the chemical inhibitors. On the other hand the adsorption mechanism can be used to study the chemical reactivity of the inhibitors. The quantum chemical indicators, such as,  $E_{\text{HOMO}}$ ,  $E_{\text{LUMO}}$ , Energy gap,  $\Delta E$  ( $E_{\text{HOMO}} - E_{\text{LUMO}}$ ), electronegativity, global softness, chemical hardness and softness and the number of electrons transferred are very important and useful parameters to study the anticorrosive effect of the investigated molecule. **Table 6** presents our computed results of the considered inhibitors in its neutral and protonated forms in both gas and aqueous phases. **Fig. 9** shows the optimized geometrical structures and the FMO surfaces (HOMO and LUMO) while the electrostatic potential maps (ESP) are presented in **Fig. 7**.

A close inspection of the optimized structure of the investigated inhibitor (**Fig. 9**) indicates that the HOMO and LUMO surfaces of the non-protonated species are distributed almost over the central part of the molecule except of the HOMO

**Table 6.** Optimized energy (in hartree), dipole moment ( $\mu^*$ ) in Debye and Quantum chemical parameters in eV of ER and HMC in both gas phase and aqueous solution.

	Gas		Solution	
	ER	HMC	ER	HMC
Energy (a.u.)	-2795.389255	-3254.345223	-2795.422351	-3254.381590
$E_{\text{HOMO}}$ (eV)	-7.211	-6.713	-7.481	-7.370
$E_{\text{LUMO}}$ (eV)	0.752	0.476	0.631	0.665
I	7.963	7.189	8.112	8.036
A	-0.752	-0.476	-0.631	-0.665
$\Delta E$	7.963	7.189	8.112	8.036
$\chi$	3.606	3.357	3.741	3.685
$\eta$	4.358	3.833	4.371	4.350
$\sigma$	0.229	0.261	0.229	0.230
$\Delta N110$	0.139	0.191	0.139	0.191
$\Delta \psi$	0.661	0.866	0.608	0.631
$\Delta E_{\text{b-d}}$	-1.089	-0.958	-1.093	-1.088

structure of the non-protonated species, in which a distribution was shown over the one of the epoxy groups. This means that the inhibitor in its both forms has a good ability to donate electron to an acceptor (metal surface). The  $E_{\text{HOMO}}$  is a measure of a molecule's tendency to receive an electron from donor species. It is well known that lower  $E_{\text{LUMO}}$  and/or higher  $E_{\text{HOMO}}$  benefit(s) higher corrosion inhibition strength [17, 18, 70, 71]. It is clearly obvious from Table 6 that the  $E_{\text{HOMO}}$  of the protonated inhibitor in aqueous medium is found to be higher than of the non-protonated species. In contrast, the value of  $E_{\text{LUMO}}$  is not in agreement with our finding.

Theoretically, another important to characterize the chemical reactivity on an inhibitor is the energy gap ( $\Delta E_{\text{gap}}$ ). Energy gap shows the capability of inhibitor to be an effective corrosion inhibitor or not [72, 73]. It was found that when the  $\Delta E_{\text{gap}}$  decreases, the adsorption efficiency between the metal surface and the inhibitors increases, because the energy to remove an electron from the HOMO must be lower [17, 18, 74].

Table 6, show that the energy break values for the non-protonated (ER) and protonated HMC species are 8.112 and 8.036 eV, respectively. The protonated form has inferior energy break ( $\Delta E_{\text{gap}}$ ) compared to the non-protonated one. This finding indicates that the adsorption performance on the steel surface of the non-protonated form is energetically favored.

Another very important, both experimental and theoretical, quantum chemical descriptor is the chemical hardness, which describes the resistance to electron cloud polarization or deformation of chemical species. Additionally, chemical hardness is a measure of the stability of the chemical molecule, which has a high energy gap. On the other hand, soft molecule, which has low energy gap can be good corrosion inhibitor in view of the fact that soft molecule can very readily give electron of HOMO to metals [17, 18, 70, 71]. An inspection of Table 7 shows that the protonated species in aqueous medium is less harder and less softer than the neutral species.

The value of  $\Delta N$  reveals the capability of the examined inhibitor to transfer its electrons to metal if  $\Delta N > 0$  and vice versa if  $\Delta N < 0$ . Based on this principle, it is apparent from the results in Table 6 that the tested inhibitor in its two forms in both gas and aqueous phases has higher propensity to give its electrons to a metal surface.

Kovacevic and Kokalj [75] introduced another important quantum parameter, which is the initial molecule-metal interaction energy ( $\Delta \psi$ ). In our work,  $\Delta \psi$  has been calculated for the investigated inhibitor in its neutral and protonated forms in both gas and aqueous phases. The results are also presented in Table 6. The results

**Table 7.** Fukui indices of the protonated (HMC) tested inhibitor in aqueous medium calculated by DFT/6-311G (d,p).

	<i>f</i> +	<i>f</i> -	<i>f</i> +	<i>f</i> -
N(1)	0.143	0.002	C(36)	0.029
N(2)	0.079	-0.002	C(40)	0.017
N(3)	0.064	0.004	C(41)	-0.009
P(4)	0.017	-0.001	C(44)	0.037
P(5)	0.016	0.005	C(48)	-0.011
P(6)	0.017	0.004	C(49)	0.019
C(7)	-0.011	-0.001	C(52)	0.036
O(10)	0.028	0.003	C(56)	0.016
O(11)	0.023	0.000	C(57)	0.032
O(12)	0.026	0.000	O(61)	0.026
O(13)	0.036	0.002	O(63)	0.050
O(14)	0.009	0.002	O(65)	0.017
O(15)	0.037	0.003	O(67)	0.023
C(16)	0.013	0.008	O(69)	-0.001
C(17)	0.011	0.007	O(71)	-0.001
C(20)	0.026	0.022	O(73)	0.019
C(24)	0.005	0.021	O(75)	0.018
C(25)	0.015	0.013	O(77)	0.012
C(28)	0.036	0.065	O(79)	0.013
C(32)	0.013	-0.002	O(81)	0.038
C(33)	0.009	0.012	O(83)	0.006

indicate that the trend of  $\Delta\psi$  is also protonated > neutral in both phases, meaning that the protonated form is better than the neutral one.

Finally, Gomez et al [44] proposed the simple charge transfer theory for donation and back-donation of charges proposed. In this theory Gomez proved that the interaction between the inhibitors and substrate surface can be probably affected by the electronic back-donation process. According to our results given in Table 6, the calculated  $\Delta E_{b-d}$  exhibits the trend: protonated > neutral in both gas and aqueous phases.

### 3.6.2. Fukui functions

The Fukui indices, in corrosion inhibition study, are an important local descriptor to investigate the relationship of the inhibitors with mild steel surface in terms of structure-activity. Herein, the current research affords an exciting chance to enhance

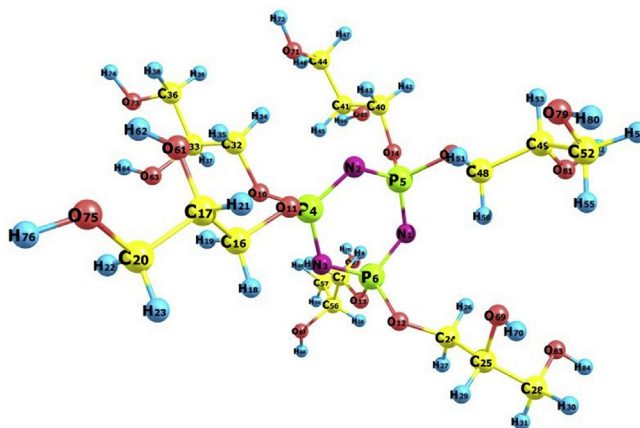


**Fig. 8.** The optimized geometrical structure of the HMC species. The indicated numbers are used for Fukui indices.

our knowledge of electron donating ability (i.e. nucleophilic  $f_k^+$ ), and electron accepting ability (i.e. electrophilic  $f_k^-$ ) of the inhibitor under probe. The Fukui indices of the protonated species of the tested inhibitor in the aqueous phase have been calculated based on the Mulliken charges by using Eqs. (14) and (15). The results are summarized in Table 7. The indicated numbers of the atoms are given Fig. 8. These results agree well the electronic distribution of the FMO orbitals (HOMO and LUMO), which were shown in Fig. 9.

### 3.7. Monte Carlo simulation

To get further information and a better understanding of how the HMC molecule behave and interact on an iron oxide surface, Monte Carlo simulation were

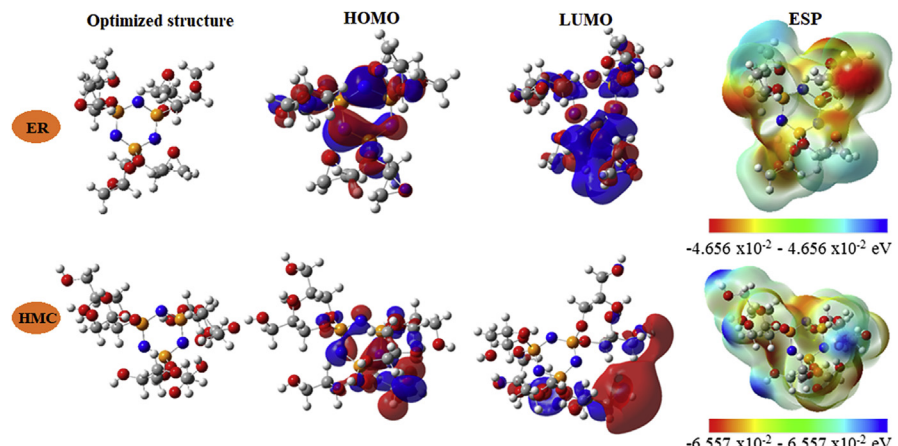


**Fig. 9.** Optimized geometrical structures, HOMO and LUMO surfaces and electrostatic potential map (ESP) of ER (non-protonated) and HMC (protonated). All values of the colored scales are in eV.

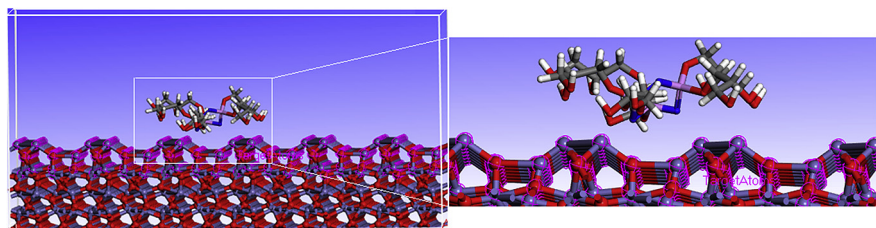


**Fig. 10.** Adsorption mode of the HMC on the Fe (110) surface.

performed on a system with the inhibitor molecule on an iron oxide  $\text{Fe}_2\text{O}_3$  surface, as presented in Fig. 10.

The strength of corrosion inhibitors absorbed on iron oxide surface can be expressed by the adsorption energy ( $E_{\text{ads}}$ ). In the present paper, the adsorption energies were calculated from the average adsorption energy of the obtained equilibrium configurations. The highest and lowest obtained  $E_{\text{ads}}$  values are -1464.57, -1442.11, kJ/mol respectively. A higher negative value of  $E_{\text{ads}}$  means that the adsorption of HMC molecule is strong, stable and therefore spontaneous adsorption on Fe (110) surface.

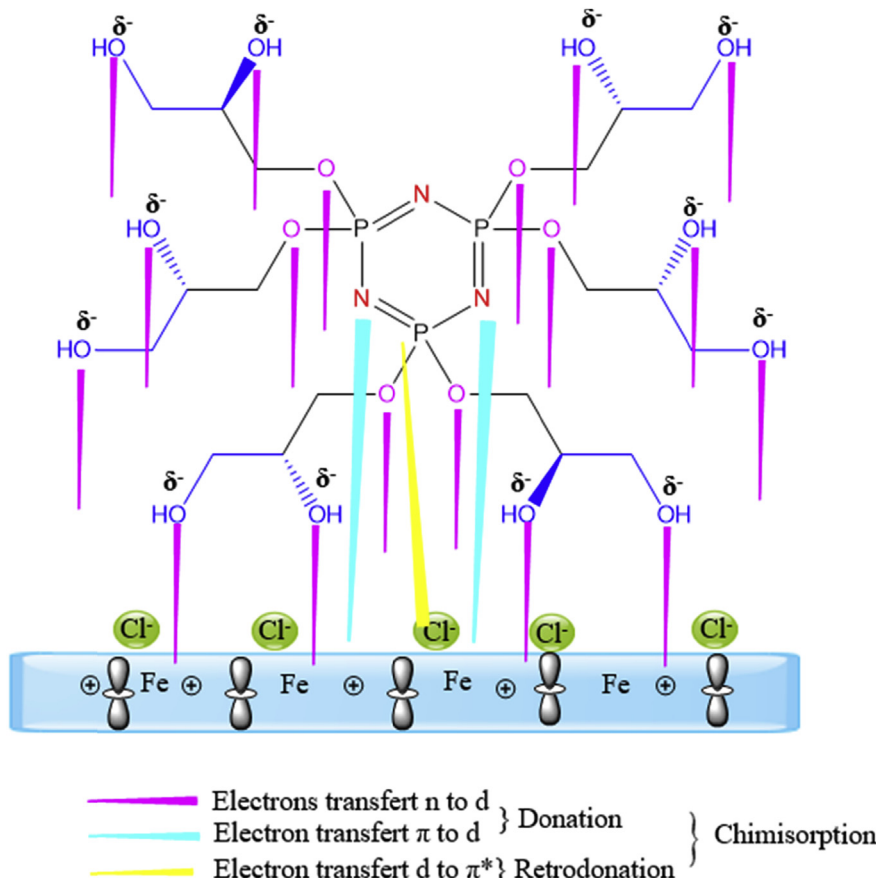


**Fig. 11.** Mechanism of HMC adsorption on carbon steel in 3% NaCl solution.

As can be seen in Fig. 10, HMC molecule is adsorbed in a parallel orientation to the metal surface through the (N, P, O) as active sites [76, 77, 78, 79,].

### 3.8. Inhibition mechanism

Experimental data, the computational calculations provided a great help in explaining the mechanism of inhibition of mode of adsorption of inhibitor and identifying the active sites. Generally, the charge on the metal, chemical structure (electronic density at the donor site) of inhibitor, type of interaction between inhibitor and metal influence the adsorption process. The HMC inhibitor has electronegative donor atoms such as nitrogen and oxygen atoms and  $\pi$ -electrons of the aromatic ring. These electron-rich donor atoms in addition with  $\pi$ -electrons of the aromatic ring favor adsorption of HMC inhibitor, thus leads to a strong interaction with the steel surface. As the observed outcome of the present investigation, HMC under goes comprehensive adsorption (involving chemisorption), the possible modes of interaction of HMC with the carbon steel surface a result of a combination of a three kinds of interactions (Fig. 11).

## 4. Conclusions

1. The synthesized Hexa (3-methoxy propan-1,2 diol) cyclotriphosphazene was significantly improved the corrosion inhibition efficiency of carbon steel in 3% NaCl, and their inhibition efficiency increases with increasing concentration.
2. The results of weight loss (WL) study were consistent with results derived from PDP and EIS studies.
3. The adsorption of HMC on the carbon steel surface from 3 % NaCl obeys a Langmuir adsorption isotherm.
4. The measurement of potentiodynamic polarization demonstrated that inhibitor HMC effectively suppressed corrosion process and classified as anodic -type inhibitor.
5. EIS studies revealed the adsorption of inhibitor and are confirmed by increase in  $R_p$  and decrease in  $C_{dl}$  values, respectively.
6. The values of  $\Delta G_{ads}^\circ$  indicating strongly interaction between inhibitor molecules and carbon steel.
7. DFT computational study shows that the inhibitive strengths of the HMC correlate with their relative reactivity and the presence of highly electronegative atoms.
8. Monte Carlo simulation suggest that the HMC molecules present a parallel adsorption model on iron substrate.

## Declarations

### Author contribution statement

Ahmed El Harfi, Mustapha El Gouri, Omar Dagdag, Zaki Safi: Conceived and designed the experiments; Performed the experiments; Analyzed and interpreted the data; Contributed reagents, materials, analysis tools or data; Wrote the paper.

Nuha Wazzan, U. Pramod Kumar, Ramzi T.T. Jalgham: Analyzed and interpreted the data.

Chandrabhan Verma, Eno Ebenso: Analyzed and interpreted the data; Wrote the paper.

### Funding statement

Chandrabhan Verma was supported by the North-West University (Mafikeng Campus) South Africa under a postdoctoral fellowship scheme.

### Competing interest statement

The authors declare no conflict of interest.

### Additional information

No additional information is available for this paper.

## References

- [1] C. Verma, M.A. Quraishi, K. Kluza, M. Makowska-Janusik, L.O. Olasunkanmi, E.E. Ebenso, Corrosion inhibition of mild steel in 1M HCl by D-glucose derivatives of dihydropyrido [2, 3-d: 6, 5-d'] dipyrimidine-2, 4, 6, 8 (1H, 3H, 5H, 7H)-tetraone, *Sci. Rep.* 7 (2017) 44432.
- [2] S.B. Aoun, On the corrosion inhibition of carbon steel in 1 M HCl with a pyridinium-ionic liquid: chemical, thermodynamic, kinetic and electrochemical studies, *RSC Adv.* 7 (58) (2017) 36688–36696.
- [3] Y. El Bakri, L. Guo, A. Harmaoui, A.B. Ali, E.M. Essassi, J.T. Mague, Synthesis, crystal structure, DFT, molecular dynamics simulation and evaluation of the anticorrosion performance of a new pyrazolotriazole derivative, *J. Mol. Struct.* 1176 (2019) 290–297.
- [4] A.A. Mahmood, I.A. Kazarinov, A.A. Khadom, H.B. Mahood, Experimental and theoretical studies of mild steel corrosion inhibition in phosphoric acid using tetrazoles derivatives, *J. Bio Tribol Corr.* 4 (4) (2018) 58.

- [5] A. Mishra, C. Verma, S. Chauhan, M.A. Quraishi, E.E. Ebenso, V. Srivastava, Synthesis, characterization, and corrosion inhibition performance of 5-aminopyrazole carbonitriles towards mild steel acidic corrosion, *J Bio Trib Corr.* 4 (4) (2018) 53.
- [6] M. Rbaa, H. Lgaz, Y. El Kacimi, B. Lakhrissi, F. Bentiss, A. Zarrouk, Synthesis, characterization and corrosion inhibition studies of novel 8-hydroxyquinoline derivatives on the acidic corrosion of mild steel: experimental and computational studies, *Mater. Dis.* 12 (2018) 43–54.
- [7] A. Singh, K.R. Ansari, J. Haque, P. Dohare, H. Lgaz, R. Salghi, M.A. Quraishi, Effect of electron donating functional groups on corrosion inhibition of mild steel in hydrochloric acid: experimental and quantum chemical study, *J. Taiwan Inst. Chem. Eng.* 82 (2018) 233–251.
- [8] A. Espinoza-Vázquez, F.J. Rodríguez-Gómez, B.I. Vergara-Arenas, L. Lomas-Romero, D. Angeles-Beltrán, G.E. Negrón-Silva, J.A. Morales-Serna, Synthesis of 1, 2, 3-triazoles in the presence of mixed Mg/Fe oxides and their evaluation as corrosion inhibitors of API 5L X70 steel submerged in HCl, *RSC Adv.* 7 (40) (2017) 24736–24746.
- [9] S. Beşli, S.J. Coles, D.B. Davies, R.J. Eaton, A. Kılıç, R.A. Shaw, Competitive formation of spiro and ansa derivatives in the reactions of tetrafluorobutane-1, 4-diol with hexachlorocyclotriphosphazene: a comparison with butane-1, 4-diol, *Polyhedron* 25 (4) (2006) 963–974.
- [10] M. El Gouri, A. El Bachiri, S.E. Hegazi, M. Rafik, A. El Harfi, Thermal degradation of a reactive flame retardant based on cyclotriphosphazene and its blend with DGEBA epoxy resin, *Polym. Degrad. Stabil.* 94 (11) (2009) 2101–2106.
- [11] S.K. Saha, M. Murmu, N.C. Murmu, I.B. Obot, P. Banerjee, Molecular level insights for the corrosion inhibition effectiveness of three amine derivatives on the carbon steel surface in the adverse medium: a combined density functional theory and molecular dynamics simulation study, *Surf. Interfaces* 10 (2018) 65–73.
- [12] O. Dagdag, A. El Harfi, O. Cherkaoui, Z. Safi, N. Wazzan, L. Guo, et al., Rheological, electrochemical, surface, DFT and molecular dynamics simulation studies on the anticorrosive properties of new epoxy monomer compound for steel in 1 M HCl solution, *RSC Adv.* 9 (8) (2019) 4454–4462.
- [13] A. Singh, K.R. Ansari, M.A. Quraishi, H. Lgaz, Y. Lin, Synthesis and investigation of pyran derivatives as acidizing corrosion inhibitors for N80 steel in hydrochloric acid: theoretical and experimental approaches, *J. Alloy. Comp.* 762 (2018) 347–362.

- [14] I. Obot, N. Obi-Egbedi, Theoretical study of benzimidazole and its derivatives and their potential activity as corrosion inhibitors, *Corros. Sci.* 52 (2010) 657–660.
- [15] S.K. Saha, M. Murmu, N.C. Murmu, P. Banerjee, Evaluating electronic structure of quinazolinone and pyrimidinone molecules for its corrosion inhibition effectiveness on target specific mild steel in the acidic medium: a combined DFT and MD simulation study, *J. Mol. Liq.* 224 (2016) 629–638.
- [16] N.A. Wazzan, I. Obot, S. Kaya, Theoretical modeling and molecular level insights into the corrosion inhibition activity of 2-amino-1, 3, 4-thiadiazole and its 5-alkyl derivatives, *J. Mol. Liq.* 221 (2016) 579–602.
- [17] Ş. Erdogan, Z.S. Safi, S. Kaya, D.Ö. Işın, L. Guo, C. Kaya, A computational study on corrosion inhibition performances of novel quinoline derivatives against the corrosion of iron, *J. Mol. Struct.* 1134 (2017) 751–761.
- [18] L. Guo, Z.S. Safi, S. Kaya, W. Shi, B. Tüzün, N. Altunay, C. Kaya, Anticorrosive effects of some thiophene derivatives against the corrosion of iron: a computational study, *Front. Chem.* 6 (2018) 155.
- [19] R.G. Pearson, Hard and soft acids and bases, *J. Am. Chem. Soc.* 85 (1963) 3533–3539.
- [20] M. Mobin, R. Aslam, Experimental and theoretical study on corrosion inhibition performance of environmentally benign non-ionic surfactants for mild steel in 3.5% NaCl solution, *Proc. Saf. Environ. Protect.* 114 (2018) 279–295.
- [21] Y. Qiang, S. Zhang, S. Xu, W. Li, Experimental and theoretical studies on the corrosion inhibition of copper by two indazole derivatives in 3.0% NaCl solution, *J. Colloid Interface Sci.* 472 (2016) 52–59.
- [22] M. Beniken, M. Driouch, M. Sfaira, B. Hammouti, M.E. Touhami, M.A. Mohsin, Anticorrosion activity of a polyacrylamide with high molecular weight on C-steel in acidic media: Part 1, *J. Bio Tribol Corr.* 4 (3) (2018) 38.
- [23] O. Dagdag, A. El Harfi, A. Essamri, M. El Gouri, S. Chraibi, M. Assouag, et al., Phosphorous-based epoxy resin composition as an effective anticorrosive coating for steel, *Int. J. Integr. Care* (2018) 1–10.
- [24] O. Dagdag, A. El Harfi, A. Essamri, A. El Bachiri, N. Hajjaji, H. Erramli, et al., Anticorrosive performance of new epoxy-amine coatings based on zinc phosphate tetrahydrate as a nontoxic pigment for carbon steel in NaCl medium, *Arabian J. Sci. Eng.* (2018) 1–11.
- [25] O. Dagdag, O. Hamed, H. Erramli, A. El Harfi, Anticorrosive performance approach combining an epoxy polyaminoamide–zinc phosphate coatings

- applied on sulfo-tartaric anodized aluminum alloy 5086, *J. Bio Tribol Corr.* 4 (4) (2018) 52.
- [26] H. Chermette, Chemical reactivity indexes in density functional theory, *J. Comput. Chem.* 20 (1999) 129–154.
- [27] M. Frisch, G. Trucks, H. Schlegel, G. Scuseria, M. Robb, J. Cheeseman, G. Scalmani, V. Barone, B. Mennucci, G. Petersson, Gaussian 09, Revision D. 01, Gaussian, Inc., Wallingford CT, 2009.
- [28] T. Keith, J. Millam, K. Eppinnett, W. Hovell, R. Semichem, Gauss View 05, Dennington II, Inc., Shawnee Mission, KS, 2005.
- [29] A.D. Becke, Density functional calculations of molecular bond energies, *J. Chem. Phys.* 84 (1986) 4524–4529.
- [30] C. Lee, W. Yang, R.G. Parr, Development of the Colle-Salvetti correlation-energy formula into a functional of the electron density, *Phys. Rev. B* 37 (1988) 785.
- [31] J. Tomasi, B. Mennucci, R. Cammi, Quantum mechanical continuum solvation models, *Chem. Rev.* 105 (2005) 2999–3094.
- [32] B. Mennucci, E. Cancès, J. Tomasi, Evaluation of solvent effects in isotropic and anisotropic dielectrics and in ionic solutions with a unified integral equation method: theoretical bases, computational implementation, and numerical applications, *J. Phys. Chem. B* 101 (1997) 10506–10517.
- [33] I. Obot, Z. Gasem, Theoretical evaluation of corrosion inhibition performance of some pyrazine derivatives, *Corros. Sci.* 83 (2014) 359–366.
- [34] R.G. Pearson, Hard and soft acids and bases—the evolution of a chemical concept, *Coord. Chem. Rev.* 100 (1990) 403–425.
- [35] R.G. Parr, R.A. Donnelly, M. Levy, W.E. Palke, Electronegativity: the density functional viewpoint, *J. Chem. Phys.* 68 (1978) 3801–3807.
- [36] R.G. Parr, R.G. Pearson, Absolute hardness: companion parameter to absolute electronegativity, *J. Am. Chem. Soc.* 105 (1983) 7512–7516.
- [37] R.G. Pearson, Absolute electronegativity and hardness: application to inorganic chemistry, *Inorg. Chem.* 27 (1988) 734–740.
- [38] P. Geerlings, F. De Proft, W. Langenaeker, Conceptual density functional theory, *Chem. Rev.* 103 (2003) 1793–1874.
- [39] R. Roy, S. Krishnamurti, P. Geerlings, S. Pal, Local softness and hardness based reactivity descriptors for predicting intra-and intermolecular

- reactivity sequences: carbonyl compounds, *J. Phys. Chem. A* 102 (1998) 3746–3755.
- [40] S. Martinez, Inhibitory mechanism of mimosa tannin using molecular modeling and substitutional adsorption isotherms, *Mater. Chem. Phys.* 77 (2003) 97–102.
- [41] A. Dutta, S.K. Saha, P. Banerjee, A.K. Patra, D. Sukul, Evaluating corrosion inhibition property of some Schiff bases for mild steel in 1 M HCl: competitive effect of the heteroatom and stereochemical conformation of the molecule, *RSC Adv.* 6 (2016) 74833–74844.
- [42] R. Wu, X. Qiu, Y. Shi, M. Deng, Molecular dynamics simulation of the atomistic monolayer structures of N-acyl amino acid-based surfactants, *Mol. Simulat.* 43 (2017) 491–501.
- [43] V. Sastri, J. Perumareddi, Molecular orbital theoretical studies of some organic corrosion inhibitors, *Corrosion* 53 (1997) 617–622.
- [44] B. Gomez, N. Likhanova, M. Dominguez-Aguilar, R. Martinez-Palou, A. Vela, J.L. Gazquez, Quantum chemical study of the inhibitive properties of 2-pyridyl-azoles, *J. Phys. Chem. B* 110 (2006) 8928–8934.
- [45] M. Bouanis, M. Tourabi, A. Nyassi, A. Zarrouk, C. Jama, F. Bentiss, Corrosion inhibition performance of 2, 5-bis (4-dimethylaminophenyl)-1, 3, 4-oxadiazole for carbon steel in HCl solution: gravimetric, electrochemical and XPS studies, *Appl. Surf. Sci.* 389 (2016) 952–966.
- [46] K. Fukui, Role of frontier orbitals in chemical reactions, *Science* 218 (1982) 747–754. <https://www.jstor.org/stable/1689733>.
- [47] K. Fukui, The Role of Frontier Orbitals in Chemical Reactions, *Frontier Orbitals and Reaction Paths: Selected Papers of Kenichi Fukui*, World Scientific, 1997, pp. 150–170.
- [48] R.K. Roy, S. Pal, K. Hirao, On non-negativity of Fukui function indices, *J. Chem. Phys.* 110 (1999) 8236–8245.
- [49] K.F. Khaled, A. El-Maghraby, Experimental, Monte Carlo and molecular dynamics simulations to investigate corrosion inhibition of mild steel in hydrochloric acid solutions, *Arabian J. Chem.* 7 (3) (2014) 319–326.
- [50] A.Y. Musa, A.A.H. Kadhum, A.B. Mohamad, M.S. Takriff, Experimental and theoretical study on the inhibition performance of triazole compounds for mild steel corrosion, *Corros. Sci.* 52 (10) (2010) 3331–3340.

- [51] M.K. Awad, M.R. Mustafa, M.M.A. Elnga, Computational simulation of the molecular structure of some triazoles as inhibitors for the corrosion of metal surface, *J. Mol. Struct. THEOCHEM* 959 (1-3) (2010) 66–74.
- [52] A.Y. Musa, R.T. Jalgham, A.B. Mohamad, Molecular dynamic and quantum chemical calculations for phthalazine derivatives as corrosion inhibitors of mild steel in 1 M HCl, *Corros. Sci.* 56 (2012) 176–183.
- [53] K.F. Khaled, Monte Carlo simulations of corrosion inhibition of mild steel in 0.5 M sulphuric acid by some green corrosion inhibitors, *J. Solid State Electrochem.* 13 (11) (2009) 1743–1756.
- [54] M.A. Mazumder, H.A. Al-Muallem, M. Faiz, S.A. Ali, Design and synthesis of a novel class of inhibitors for mild steel corrosion in acidic and carbon dioxide-saturated saline media, *Corros. Sci.* 87 (2014) 187–198.
- [55] H. Ashassi-Sorkhabi, E. Asghari, Effect of hydrodynamic conditions on the inhibition performance of l-methionine as a “green” inhibitor, *Electrochim. Acta* 54 (2008) 162–167.
- [56] H. Jamil, M.F. Montemor, R. Boulif, A. Shriri, M.G.S. Ferreira, An electrochemical and analytical approach to the inhibition mechanism of an amino-alcohol-based corrosion inhibitor for reinforced concrete, *Electrochim. Acta* 48 (23) (2003) 3509–3518.
- [57] M.B. Valcarce, M. Vázquez, Carbon steel passivity examined in solutions with a low degree of carbonation: the effect of chloride and nitrite ions, *Mater. Chem. Phys.* 115 (1) (2009) 313–321.
- [58] R. Solmaz, G. Kardaş, M. Culha, B. Yazıcı, M. Erbil, Investigation of adsorption and inhibitive effect of 2-mercaptopthiazoline on corrosion of mild steel in hydrochloric acid media, *Electrochim. Acta* 53 (20) (2008) 5941–5952.
- [59] S.K. Saha, A. Dutta, P. Ghosh, D. Sukul, P. Banerjee, Novel Schiff-base molecules as efficient corrosion inhibitors for mild steel surface in 1 M HCl medium: experimental and theoretical approach, *Phys. Chem. Chem. Phys.* 18 (27) (2016) 17898–17911.
- [60] S. John, A. Joseph, Theoretical and electrochemical studies on the effect of substitution on 1, 2, 4-triazole towards mild steel corrosion inhibition in hydrochloric acid, *Indian J. Chem. Technol.* 19 (3) (2012) 195–204.
- [61] S. Pareek, D. Jain, S. Hussain, A. Biswas, R. Shrivastava, S.K. Parida, et al., A new insight into corrosion inhibition mechanism of copper in aerated 3.5%(by weight) NaCl solution by eco-friendly imidazopyrimidine dye: experimental and theoretical approach, *Chem. Eng. J.* (2018).

- [62] R.T. Loto, O. Tobilola, Corrosion inhibition properties of the synergistic effect of 4-hydroxy-3-methoxybenzaldehyde and hexadecyltrimethylammonium bromide on mild steel in dilute acid solutions, *J. King Saud Univ. Eng. Sci.* (2016).
- [63] M. Galai, M. El Gouri, O. Dagdag, Y. El Kacimi, A. Elharfi, M. Ebn Touhami, New hexa propylene glycol cyclotiphosphazene as efficient organic inhibitor of carbon steel corrosion in hydrochloric acid medium, *J. Mater. Environ. Sci.* 7 (2016) 1562.
- [64] I.B. Obot, S.A. Umoren, Z.M. Gasem, R. Suleiman, B. El Ali, Theoretical prediction and electrochemical evaluation of vinylimidazole and allylimidazole as corrosion inhibitors for mild steel in 1 M HCl, *J. Ind. Eng. Chem.* 21 (2015) 1328–1339.
- [65] A. Salhi, S. Tighadouini, M. El-Massaoudi, M. Elbelghiti, A. Bouyanzer, S. Radi, et al., Keto-enol heterocycles as new compounds of corrosion inhibitors for carbon steel in 1 M HCl: weight loss, electrochemical and quantum chemical investigation, *J. Mol. Liq.* 248 (2017) 340–349.
- [66] M. Elfaydy, R. Touir, M. Ebntouhami, A. Zarrouk, C. Jama, B. Lakhrissi, et al., Corrosion inhibition performance of newly synthesized 5-alkoxymethyl-8-hydroxyquinoline derivatives for carbon steel in 1 M HCl solution: experimental, DFT and Monte Carlo simulation studies, *Phys. Chem. Chem. Phys.* (2018).
- [67] T. Douadi, H. Hamani, D. Daoud, M. Al-Noaimi, S. Chafaa, Effect of temperature and hydrodynamic conditions on corrosion inhibition of an azomethine compounds for mild steel in 1 M HCl solution, *J. Taiwan Inst. Chem. Eng.* 71 (2017) 388–404.
- [68] N.U. Inbaraj, G.V. Prabhu, Corrosion inhibition properties of paracetamol based benzoxazine on HCS and Al surfaces in 1M HCl, *Prog. Org. Coating* 115 (2018) 27–40.
- [69] A. Bouoidina, F. El-Hajjaji, M. Drissi, M. Taleb, B. Hammouti, I.M. Chung, et al., Towards a deeper understanding of the anticorrosive properties of hydrazine derivatives in acid medium: experimental, DFT and MD simulation assessment, *Metall. Mater. Trans.* (2018) 1–12.
- [70] I. Danaee, O. Ghasemi, G. Rashed, M.R. Avei, M. Maddahy, Effect of hydroxyl group position on adsorption behavior and corrosion inhibition of hydroxybenzaldehyde Schiff bases: electrochemical and quantum calculations, *J. Mol. Struct.* 1035 (2013) 247–259.

- [71] F. El-Hajjaji, M. Messali, A. Aljuhani, M. Aouad, B. Hammouti, M. Belghiti, D. Chauhan, M. Quraishi, Pyridazinium-based ionic liquids as novel and green corrosion inhibitors of carbon steel in acid medium: electrochemical and molecular dynamics simulation studies, *J. Mol. Liq.* 249 (2018) 997–1008.
- [72] R. Kumar, S. Chahal, S. Kumar, S. Lata, H. Lgaz, R. Salghi, S. Jodeh, Corrosion inhibition performance of chromone-3-acrylic acid derivatives for low alloy steel with theoretical modeling and experimental aspects, *J. Mol. Liq.* 243 (2017) 439–450.
- [73] L. Afia, O. Hamed, M. Larouj, H. Lgaz, S. Jodeh, R. Salghi, Novel natural based diazepines as effective corrosion inhibitors for carbon steel in HCl solution: experimental, theoretical and Monte Carlo simulations, *Trans. Indian Inst. Met.* 70 (2017) 2319–2333.
- [74] S. Deng, X. Li, X. Xie, Hydroxymethyl urea and 1, 3-bis (hydroxymethyl) urea as corrosion inhibitors for steel in HCl solution, *Corros. Sci.* 80 (2014) 276–289.
- [75] N. Kovačević, A. Kokalj, Analysis of molecular electronic structure of imidazole-and benzimidazole-based inhibitors: a simple recipe for qualitative estimation of chemical hardness, *Corros. Sci.* 53 (2011) 909–921.
- [76] K.F. Khaled, M.A. Amin, Corrosion monitoring of mild steel in sulphuric acid solutions in presence of some thiazole derivatives—molecular dynamics, chemical and electrochemical studies, *Corros. Sci.* 51 (9) (2009) 1964–1975.
- [77] S. Xia, M. Qiu, L. Yu, F. Liu, H. Zhao, Molecular dynamics and density functional theory study on relationship between structure of imidazoline derivatives and inhibition performance, *Corros. Sci.* 50 (7) (2008) 2021–2029.
- [78] A. Mishra, C. Verma, V. Srivastava, H. Lgaz, M.A. Quraishi, E.E. Ebenso, I.M. Chung, Chemical, electrochemical and computational studies of newly synthesized novel and environmental friendly heterocyclic compounds as corrosion inhibitors for mild steel in acidic medium, *J. Bio Tribol Corr.* 4 (3) (2018) 32.
- [79] D. Wang, B. Xiang, Y. Liang, S. Song, C. Liu, Corrosion control of copper in 3.5 wt.% NaCl solution by domperidone: experimental and theoretical study, *Corros. Sci.* 85 (2014) 77–86.